Interactions of Two Porphyrin Rings: Metal-Induced Structural Change of 5,5′-Ethylenebis(porphyrin)

Ken-ichi Sugiura, Gelii Ponomarev,† Satoshi Okubo,†† and Akio Tajiri,††† and Yoshiteru Sakata*

The Institute of Scientific and Industrial Research, Osaka University, Mihoga-oka 8-1, Ibaraki, Osaka 567

†Institute of Biophysics of Russian Ministry of Health, Moscow 123182, Russia

††Hachinohe National College of Technology, Hachinohe 036

†††Department of Chemistry, College of Education, Hirosaki University, Hirosaki 036

(Received November 18, 1996)

5,5′-Ethylenebis(octaethylporphyrin) **1** and its metallocomplexes with various combination of metals (Zn, Cu, and Ni) **2**—**10** were prepared. On the basis of ^{1}H and ^{13}C NMR as well as MCD spectra, it was concluded that interactions between the two intramolecular porphyrins become attractive when at least one of the two rings is converted to zinc porphyrin. The phenomenon was explained by dipole–dipole interaction arising from the large polarization in Zn complexes.

Stacking interaction is seen in various π-systems[1] and is important especially in porphyrin rings in connection with the special pair at the photosynthetic reaction center.[2] The nature of the π–π interaction between two faced porphyrins was studied theoretically and is explained by attractive interactions between a positively charged σ-framework of one porphyrin ring and some other negatively charged π-system.[3] Such phenomena have been observed intramolecularly in solution as well as in solid state[4—8] and intramolecularly in covalently linked dimer systems.[9—13]

Since a porphyrin ring can be coordinated by various metal ions, stacking interactions in porphyrins are expected to vary with a change of the central metal. However, systematic studies on this problem have not been carried out, because of the lack of suitable compounds to evaluate the interaction. For such a study, a new type of porphyrin dimer is required. As a good candidate, we chose Arnold's porphyrin dimer **1**[14,15] in which two octaethylporphyrin (OEP) rings are linked by a flexible ethylene chain. It is expected that this compound will adopt a *syn* or *anti* conformation depending upon attractive or repulsive interaction between the two metalloporphyrin rings (Fig. 1). Bearing these possibilities in mind, we synthesized **1** as well as the corresponding metallocomplexes **2**—**10** and studied their conformational changes with a change of inserted metals (Charts 1 and 2).

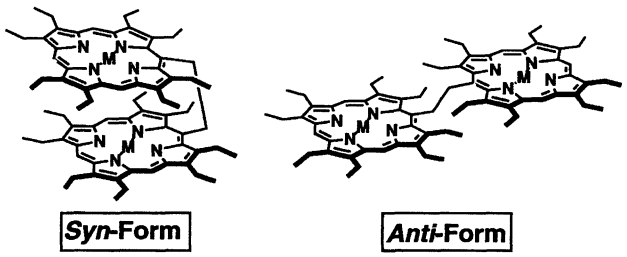

Fig. 1. Two major conformations, *syn*- and *anti*-, for 5,5′-ethylenbis(octaethylporphyrin).

Experimental

General. NMR spectra were obtained with a JEOL EX-270 (270 MHz for ^{1}H NMR 67.5 MHz for ^{13}C NMR) using TMS as an internal standard. 1D and 2D experiments were performed with

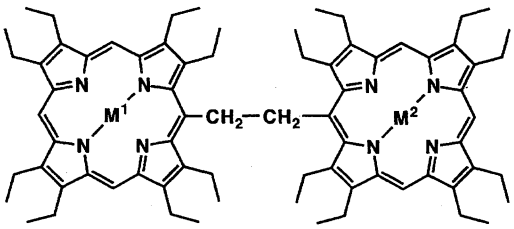

1 (M^1 = M^2 = 2H)
2 (M^1 = 2H, M^2 = Ni)
3 (M^1 = 2H, M^2 = Cu)
4 (M^1 = 2H, M^2 = Zn)
5 (M^1 = Ni, M^2 = Ni)
6 (M^1 = Ni, M^2 = Cu)
7 (M^1 = Ni, M^2 = Zn)
8 (M^1 = Cu, M^2 = Cu)
9 (M^1 = Cu, M^2 = Zn)
10 (M^1 = Zn, M^2 = Zn)

Chart 1.

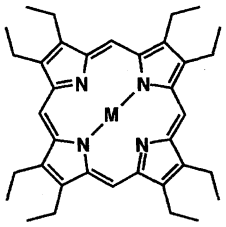

11 (M = 2H)
12 (M = Ni)
13 (M = Cu)
14 (M = Zn)

Chart 2.

standard JEOL puls sequences. DQF-COSY was obtained for a 2048×512 matrix, 1.16 Hz digital resolution, and zero filled to 1024 in the F1 direction. The 2D NOESY was recorded in the phase-sensitive mode, a 1.00 second mixing time led to the best map. HMBC was obtained for a 2048×512 matrix and zero filled 1024 in the F1 direction.

Absorption spectra were obtained with a Hitachi 260-70 spectrometer. MCD spectra were recorded on a JASCO J-20 and a JASCO-500C recording circular dichrometers equipped with an 11.7 kG electromagnet.

5,5′-Ethylenbis(octaethylporphyin) 1 (M^1=M^2=2H).[15] A mixture of 6.29 g (10.2 mmol) of [5-(hydoxymethyl)octaethylporphyrinato]nickel,[15] 3.11 g of concd sulfuric acid, and 300 mL of DMF was stirred under reflux for 1 h. After being cooled to room temperature, the mixture was poured into ice water. The precipitated crude product was collected and washed with water. Without further purification, the crude product was stirred in 10 mL of concd sulfuric acid for 2 h at room temperature and poured onto ice water. After being neutralized with aqueous sodium hydrogencarbonate, the mixture was extracted with 3×300 mL of CH_2Cl_2 and washed with water. The solvent was removed by rotary evaporation and the crude product was chromatographed on SiO_2. The second main brown fraction was collected and recrystallized from toluene to give **1**, 3.83 g, 69%, mp > 300°C. Anal. Calcd for $C_{74}H_{94}N_8$: C, 81.12; H, 8.65; N, 10.23%. Found: C, 81.32; H, 8.41; N, 10.37%.

UV-vis λ_{abs} ($CHCl_3$) 285 (sh, log ε = 4.21), 332 (sh, 4.49), 417 (5.36), 515 (4.44), 550 (4.07), 585 (4.08), and 638 nm (3.48). ^{1}H NMR ($CDCl_3$) δ = 9.87 (s, 2H, H^{15}), 9.79 (s, 4H, H^{10} and H^{20}), 5.00 (s, 4H, H^{37}), 4.09 (q, J = 7.59 Hz, 8H, CH_2 of Et-D), 4.07 (q, J = 7.59 Hz, 8H, CH_2 of Et-C), 3.74 (br q, J = 7.59 Hz, 8H, CH_2 of Et-B), 3.52 (br q, J = 7.59 Hz, 8H, CH_2 of Et-A), 1.94 (q, J = 7.59 Hz, 12H, CH_3 of Et-D), 1.92 (t, J = 7.59 Hz, 12H, CH_3 of Et-C), 1.67 (t, J = 7.59 Hz, 12H, CH_3 of Et-B), 1.11 (t, J = 7.59 Hz, 12H, CH_3 of Et-A), −2.83 (br s, 2H), and −3.06 (br s, 2H). ^{13}C NMR ($CDCl_3$) δ = 145.1 (C^{13} and C^{17}), 144.3 (C^4 and C^6), 143.4 (C^2 and C^8), 142.6 (C^{11} and C^{19}), 141.7 (C^{12} and C^{18}), 141.0 (C^1 and C^9), 140.7 (C^{14} and C^{16}), 140.3 (C^3 and C^7), 117.0 (C^5), 96.4 (C^{10} and C^{20}), 95.5 (C^{15}), 39.0 (C^{37}), 22.4 (C^{23} and C^{25}), 19.8 (C^{29}, C^{31}, C^{33}, and C^{35}), 19.6 (C^{21} and C^{27}), 18.5 (C^{30}, C^{32}, C^{34}, and C^{36}), 18.2 (C^{22} and C^{28}), and 17.8 (C^{24} and C^{26}). ^{1}H and ^{13}C NMR peak assignments were made on the basis of 2D NMR experiments.

Dimer 5 (M^1=M^2=Ni).[15] A mixture of **1** (50.0 mg, 45.6 μmol) and nickel acetate tetrahydrate (570.0 mg, 2.29 mmol) in chloroform (20 mL) was stirred for 24 h under reflux. After the solvent was removed under reduced pressure, the crude product was chromatographed on SiO_2 using toluene eluent. Crystallization from toluene gave 39.8 mg (72%) of **5**, mp > 300°C.

UV-vis λ_{max} ($CHCl_3$) 250 (sh, log ε = 4.48), 302 (4.33), 347 (4.39), 410 (sh, 5.28), 419 (5.31), 539 (4.28), and 574 nm (4.33). ^{1}H NMR ($CDCl_3$) δ = 9.48 (s, 2H, H^{15}), 9.32 (s, 4H, H^{10} and H^{20}), 4.0—3.7 (m, 16H, CH_2 of Et-C and Et-D), 3.88 (s, 4H, H^{37}), 3.60 (br q, 8H, CH_2 of Et-A), 3.00 (br q, 8H, CH_2 of Et-A), 1.86 (t, J = 7.59 Hz, 12H, CH_3 of Et-D), 1.80 (t, J = 7.59 Hz, 12H, CH_3 of Et-C), 1.61 (t, J = 7.59 Hz, 12H, CH_3 of Et-B), and 1.05 (t, J = 7.59 Hz, 12H, CH_3 of Et-A). ^{13}C NMR ($CDCl_3$) δ = 145.4, 143.7, 142.8, 142.6, 140.0, 139.4, 139.3, 137.8, 112.8, 96.5, 95.7, 22.1, 19.7, 19.6, 19.3, 18.2, 18.1, 18.0, and 17.7.

Dimer 8 (M^1=M^2=Cu).[15] A solution containing **1** (22.4 mg, 20.4 μmol) and copper acetate monohydrate (81.5 mg, 410 mmol) in 10 mL chloroform was refluxed for 10 min. The reaction mixture was chromatographed on SiO_2 to afford 22.0 mg (93%) of the dimer **8**. The crude product was recrystallized from heptane, mp > 300°C. Anal. Calcd for $C_{74}H_{90}Cu_2N_8$: C, 72.93; H, 7.44; N, 9.19%. Found: C, 72.72; H, 7.58; N, 8.99%.

UV-vis λ_{max} ($CHCl_3$) 327 (log ε = 4.51), 396 (5.36), 406 (5.31), 421 (sh, 5.11), 546 (4.27), 578 (4.21) and 588 (4.18) nm.

Dimer 10 (M^1=M^2=Zn). A procedure similar to that described above was used for the synthesis of **10** starting from 34.2 mg of **1** and 100.0 mg of zinc acetate dihydrate in 10 mL of chloroform with reflux. The yield was quantitative. The crude product was recrystallized from heptane and gave 32.0 mg (84%) of **10**, mp > 300°C. Anal. Calcd for $C_{74}H_{90}N_8Zn_2$: C, 72.72; H, 7.42; N, 9.13%. Found: C, 72.77; H, 7.37; N, 9.30%.

UV-vis λ_{max} ($CHCl_3$) 320 (sh, log ε = 4.59), 397 (5.42), 553 (4.23), 582 (4.05) and 592 (4.03) nm. λ_{max} ($CHCl_3$ with one drop of pyridine) 423 (log ε = 5.48), 437 (5.47), 560 (4.53), and 598 (4.02) nm. ^{1}H NMR ($CDCl_3$) δ = 9.84 (s, 2H, H^{15}), 8.17 (s, 4H, H^{10} and H^{20}), 5.19 (s, 4H, H^{37}), 4.30 (dt, J = 7.26 and −15.0 Hz, $H^{31'}$ and $H^{33'}$), 4.11 (dt, J = 7.26 and −15.0 Hz, H^{31} and H^{33}), 3.90 (dt, J = 7.26 and −15.0 Hz, $H^{29'}$ and $H^{35'}$), 3.72 (dt, J = 7.26 and −15.0 Hz, H^{29} and H^{35}), 3.35 (dt, J = 7.26 and −15.0 Hz, H^{23} and H^{25}), 3.11 (dt, J = 7.26 and −15.0 Hz, $H^{23'}$ and $H^{25'}$), 2.64 (dt, J = 7.26 and −15.0 Hz, H^{21} and H^{27}), 2.36 (dt, J = 7.26 and −15.0 Hz, $H^{21'}$ and $H^{27'}$), 1.95 (t, J = 7.26 Hz, H^{32} and H^{34}), 1.65 (t, J = 7.26 Hz, H^{30} and H^{36}), 1.44 (t, J = 7.26 Hz, H^{24} and H^{26}), and 1.07 (t, J = 7.26 Hz, H^{22} and H^{28}); (C_6D_5Cl) δ = 9.97 (s, 2H), 8.38 (s, 4H), 5.38 (s, 4H), 4.31 (dt, J = 7.26 and −15.0 Hz), 4.06 (dt, J = 7.26 and −15.0 Hz), 3.89 (dt, J = 7.26 and −15.0 Hz), 3.83 (dt, J = 7.26 and −15.0 Hz), 3.52 (dt, J = 7.26 and −15.0 Hz), 3.23 (dt, J = 7.26 and −15.0 Hz), 2.83 (dt, J = 7.26 and −15.0 Hz), 2.57 (dt, J = 7.26 and −15.0 Hz), 1.98 (dt, J = 7.26 Hz), 1.72 (t, J = 7.26 Hz), 1.51 (t, J = 7.26 Hz), and 1.20 (t, J = 7.26 Hz). ^{13}C NMR ($CDCl_3$) δ = 147.0 (C^{14} and C^{16}), 146.1 (C^4 and C^6), 145.6 (C^{11} and C^{19}), 142.7 (C^1 and C^9), 141.7 (C^2 and C^8), 141.2 (C^{12} and C^{18}), 140.9 (C^{13} and C^{17}), 139.9 (C^3 and C^7), 116.9 (C^5), 96.0 (C^{15}), 95.5 (C^{10} and C^{20}), 39.0 (C^{37}), 22.4 (C^{23} and C^{25}), 20.0 (C^{31} and C^{33}), 19.6 (C^{29} and C^{35}), 18.7 (C^{32} and C^{34}), 18.5 (C^{30} and C^{36}), 18.3 (C^{21} and C^{27}), 17.8 (C^{24} and C^{26}), and 17.6 (C^{22} and C^{28}). ^{1}H and ^{13}C NMR peak assignments were made on the basis of 2D NMR experiments.

Dimer 2 (M^1=2H, M^2=Ni). A mixture of **1** (153.0 mg, 140 μmol) and nickel acetate tetrahydrate (51.9 mg, 209 μmol) in 30 mL of chloroform was refluxed for 6 h. The solvent was removed under reduced pressure and the residue was chromatographed on SiO_2 using toluene as an eluent. The first band contained di-metallated complex **5**, 23.0 mg, 14%.The second main band was eluted with chloroform to yield 86.3 mg (54%) of **2**; mp > 300°C. Anal. Calcd for $C_{74}H_{92}N_8Ni$: C, 77.13; H, 8.05; N, 9.72%. Found: C, 76.89; H, 8.07; N, 9.62%.

UV-vis λ_{max} ($CHCl_3$) 312 (sh, log ε = 4.32), 420 (5.36), 515 (4.27), 544 (4.21), 581 (4.22), and 637 (2.26) nm. ^{1}H NMR ($CDCl_3$) δ = 9.98 (s, 2H), 9.90 (s, 1H), 9.56 (s, 1H), 9.38 (s, 2H), 4.52 (br t, 2H), 4.48 (br t, 2H), 4.14 (q, J = 7.26 Hz, 4H), 4.11 (q, J = 7.26 Hz, 4H), 3.95—3.87 (m, 2H), 3.69 (q, J = 7.26 Hz, 4H), 3.37 (q, J = 7.26 Hz, 4H), 3.34 (q, J = 7.26 Hz, 4H), 1.98 (t, J = 7.26 Hz, 6H), 1.96 (t, J = 7.26 Hz, 6H), 1.92 (t, J = 7.26 Hz, 6H), 1.86 (t, J = 7.26 Hz, 6H), 1.80 (t, J = 7.26 Hz, 6H), 1.69 (t, J = 7.26 Hz, 6H), 1.15 (t, J = 7.26 Hz, 6H), 1.10 (t, J = 7.26 Hz, 6H), −2.79 (bs, 1H), −2.90 (bs, 1H). ^{13}C NMR ($CDCl_3$) δ = 145.4, 145.2, 144.3, 143.8, 143.5, 142.8, 142.7, 141.8, 141.2, 140.8, 140.3, 140.1, 139.5, 139.4, 137.8, 96.6, 96.5, 95.8, 95.6, 22.4, 22.3, 19.8, 19.7, 19.6, 19.5, 18.5, 18.4, 18.2, 18.0, 17.9, and 17.7.

Dimer 3 (M^1=2H, M^2=Cu). A mixture of **1** (172.0 mg, 157 μmol) and copper acetate monohydrate (53.9 mg, 271 μmol) in 50 mL of chloroform was stirred at room temperature for about 30 min.

The reaction mixture was charged on the top of SiO_2 column directly and eluted with chloroform as soon as possible to remove unreacted copper acetate and to avoid further metallation. The eluted mixture of di- and mono-metalated complexes was concentrated to dryness and chromatographed on SiO_2 once more. The first band eluted with toluene contained di-metallated complex **8**, 32.0 mg (18% yield). The second main band was eluted with chloroform to yield 89.0 mg (49%) of **3**, mp > 300°C. Anal. Calcd for $C_{74}H_{92}CuN_8$: C, 76.81; H, 8.01; N, 9.68%. Found: C, 76.54; H, 7.89; N, 9.40%.

UV-vis λ_{max} ($CHCl_3$) 334 (log ε = 4.51), 398 (sh, 5.26), 410 (5.32), 421 (sh, 5.26), 516 (4.18), 547 (4.21), 586 (4.15), and 639 (3.23) nm.

Dimer 4 (M^1=2H, M^2=Zn). A procedure similar to that described for **3** was used for the synthesis of **4** starting from 22.2 mg of **1**, 19.6 mg of zinc acetate dihydrate, 10 mL of chloroform at room temperature to yield 12.4 mg (49%) of **4** together with 5.8 mg (22%) of **10**. The crude product was recrystallized from heptane, mp > 300°C.

UV-vis λ_{max} ($CHCl_3$) 334 (sh, log ε = 4.55), 403 (5.24), 514 (4.08), 550 (4.17), 588 (4.02), and 640 (3.23) nm. λ_{max} ($CHCl_3$ with one drop of pyridine) 345 (sh, log ε = 4.47), 429 (5.47), 514 (4.22), 556 (4.28), 580 (sh, 4.05), 600 (sh, 3.89), and 638 (3.15) nm. ^{1}H NMR ($CDCl_3$) δ = 9.84 (s, 1H), 9.72 (s, 1H), 8.77 (s, 2H), 8.71 (s, 2H), 5.31 (t, J = 5.94 Hz, 2H), 5.00 (t, J = 5.94 Hz, 2H), 4.30—4.00 (m, 8H), 4.00—3.80 (m, 4H), 3.80—3.65 (m, 4H), 3.51 (dt, J = 7.59, −15.0 Hz, 2H), 3.39 (dt, J = 7.59, −15.0 Hz, 2H), 3.25—3.10 (m, 4H), 3.10—2.90 (m, 4H), 2.90—2.65 (m, 4H), 1.95 (t, J = 7.59 Hz, 6H), 1.93 (t, J = 7.59 Hz, 6H), 1.73 (t, J = 7.59 Hz, 6H), 1.72 (t, J = 7.59 Hz, 6H), 1.45 (t, J = 7.59 Hz, 12H), 1.23 (t, J = 7.59 Hz, 6H), 1.14 (t, J = 7.59 Hz, 6H), and −4.37 (bs, 2H). ^{13}C NMR ($CDCl_3$) δ = 147.0, 146.9, 146.1, 144.7, 144.0, 143.0, 142.7, 141.6, 141.5, 141.4, 141.3, 141.1, 140.4, 139.9, 139.2, 138.9, 116.7, 116.3, 96.2, 96.0, 95.3, 94.9, 22.7, 22.0, 20.0, 19.8 (two kinds of carbons), 19.7, 19.6, 19.0, 18.7, 18.5 (three kinds of carbons), 18.4, 18.2, 17.9, 17.7 (two kinds of carbons), 17.6, and 17.3.

Dimer 6 (M^1=Ni, M^2=Cu). A mixture of **2** (50.0 mg, 43 μmol) and copper acetate monohydrate (100.0 mg, 503 μmol) in 20 mL of chloroform was stirred for 15 min at room temperature. The solvent was removed under reduced pressure. The crude product was chromatographed on SiO_2 using chloroform as an eluent and recrystallized from heptane to give 47.0 mg (89% yield) of **6**, mp > 300°C. Anal. Calcd for $C_{74}H_{90}CuN_8Ni$: C, 73.22; H, 7.47; N, 9.23%. Found: C, 72.60; H, 6.75; N, 9.34%.

UV-vis λ_{max} ($CHCl_3$) 310 (log ε = 4.35), 332 (4.43), 414 (5.36), 421 (5.36), 500 (sh, 3.85), 541 (4.34), and 574 (4.32) nm.

Dimer 7 (M^1=Ni, M^2=Zn). The synthesis of **7** was carried out in a manner similar to that described for **6**. The crude product was recrystallized from heptane and gave 94% yield of **7**: Mp > 300°C. Anal. Calcd for $C_{74}H_{90}CuN_8Zn$: C, 72.82; H, 7.43; N, 9.18%. Found: C, 72.85; H, 7.38; N, 9.14%.

UV-vis λ_{max} ($CHCl_3$) 310 (log ε = 4.30), 348 (4.44), 413 (5.25), 423 (5.26), 547 (4.28), and 576 nm (4.19). λ_{max} ($CHCl_3$ with one drop of pyridine) 340 (log ε = 4.48), 411 (sh, 5.21), 428 (5.44), and 560 nm(4.35). ^{1}H NMR ($CDCl_3$) δ = 9.95 (s, 1H), 9.46 (s, 1H), 9.44 (s, 2H), 8.70 (s, 2H), 4.61 (t, J = 6.70 Hz, 2H), 4.47 (t, J = 6.70 Hz, 2H), 4.25—4.00 (m, 8H), 3.95 (q, J = 7.59 Hz, 4H), 3.70 (q, J = 7.59 Hz, 4H), 3.45—3.30 (m, 4H), 3.30—3.10 (m, 4H), 3.10—2.95 (m, 8H), 1.96 (t, J = 7.59 Hz, 6H), 1.87 (t, J = 7.59 Hz, 6H), 1.86 (t, J = 7.59 Hz, 6H), 1.64 (t, J = 7.59 Hz, 6H), 1.53 (t, J = 7.59 Hz, 6H), 1.31 (t, J = 7.59 Hz, 6H), 1.18 (t, J = 7.59 Hz, 6H), and 1.14 (t, J = 7.59 Hz, 6H).

Dimer 9 (M^1=Cu, M^2=Zn). The synthesis of **9** was carried out in a manner similar to that described for **6**. The crude product was recrystallized from heptane and gave 84% yield of **9**: Mp > 300°C.

UV-vis λ_{max} ($CHCl_3$) 329 (log ε = 4.54), 396 (5.40), 409 (sh, 5.27), 422 (sh, 5.02), 550 (4.25), 580 (4.13), and 590 (sh, 4.10) nm.

21*H*,23*H*-Octaethylporphyrin (2HOEP) 11. The reference OEPs were prepared by the reported methods.[16,17] UV-vis λ_{max} ($CHCl_3$) 269 (log ε = 3.78), 333 (sh, 4.14), 353 (sh, 4.43), 378 (4.84), 398 (5.12), 498 (4.02), 502 (3.99), 533 (3.90), 566 (3.72), 594 (3.06), and 620 nm (3.58). ^{1}H NMR ($CDCl_3$) δ = 10.10 (s, 4H), 4.11 (q, J = 7.59 Hz, 16H), 1.92 (t, J = 7.59 Hz, 24H), and −3.74 (bs, 2H). ^{13}C NMR ($CDCl_3$) δ = 144.0 (br), 141.4, 96.4, 19.8, and 18.6.

(Octaethylporphyrinato)nickel (NiOEP) 12. ^{1}H NMR ($CDCl_3$) δ = 9.76 (s, 4H), 3.93 (q, J = 7.59 Hz, 16H), and 1.82 (t, J = 7.59 Hz, 24H). ^{13}C NMR ($CDCl_3$) δ = 142.5, 140.4, 96.8, 19.7, and 18.3 ppm.

CuOEP 13. UV-vis λ_{max} ($CHCl_3$) 287 (sh, log ε = 3.82), 325 (4.33), 380 (sh, 4.78), 397 (5.66), 490 (sh, 3.51), 523 (4.21), and 560 (4.51) nm.

ZnOEP 14. UV-vis λ_{max} ($CHCl_3$) 329 (log ε = 4.27), 352 (sh, 4.28), 382 (sh, 4.72), 400 (5.54), 498 (sh, 3.34), 531 (4.19), and 567 (4.36). λ_{max} ($CHCl_3$ with one drop of pyridine) 333 (log ε = 4.42), 394 (sh, 4.75), 413 (5.53), 541 (4.23), and 577 (4.14) nm. ^{1}H NMR ($CDCl_3$) δ = 10.17 (s, 4H), 4.13 (q, J = 7.59 Hz, 16H), and 1.95 (t, J = 7.59 Hz, 24H); ($CDCl_3$ with one drop of pyridine-d_5) δ = 10.04 (s, 4H), 4.10 (q, J = 7.59 Hz, 16H), and 1.90 (t, J = 7.59 Hz, 24H). ^{13}C NMR ($CDCl_3$) δ = 147.5, 142.3, 97.4, 19.9, and 18.7.

Results

Synthesis. Free base dimer porphyrin **1** was prepared by an acid-catalyzed coupling reaction[15,18] of [5-(hydroxymethyl)octaethylporphyrinato]nickel. Separation of pure **5** from the by-product of (5-methyloctaethylporphyrinato)nickel was difficult by the usual column chromatography. However, this impurity was easily removed from dimer **1** after demetalation reaction of the mixture. Di-metal complexes were obtained by the usual metal acetate method.[17] Mixed metal complexes were prepared by considering the stability constants of metal porphyrins.[19,20] At first, mono-metalated complexes **2**, **3**, and **4** were prepared in moderate yield by the usual metal acetate method[17] under strictly controlled reaction conditions. The half-metalated complexes **2** and **3** were treated with appropriate metal acetates to give mixed metal complexes, **6**, **7**, and **9** (Scheme 1). No transmetalation reaction in mixed metal complexes could be detected by TLC under these reaction conditions. Various attempts to prepare magnesium-containing complexes remained unsuccessful.[21]

NMR Spectroscopy. ^{1}H NMR spectra of all the dimers and references except paramagnetic Cu complexes **3**, **6**, **8**, **9**, and **13** were measured in $CDCl_3$ and/or chlorobenzene-d_5. No concentration dependence of the chemical shifts of these compounds was observed in $CDCl_3$ in the range of 1 mM to saturated solution (ca. 10 mM) indicating that intermolecular interaction may be excluded although the low solubility of the complexes prevents us from estimating detailed solvent effects. A typical example of the spectra is shown in Fig. 2 for **1** and **10**. In Fig. 2 there are two characteristic features for **10**. First, methylene protons of ethyl substituents were observed as non equivalent signals. Second, an upfield

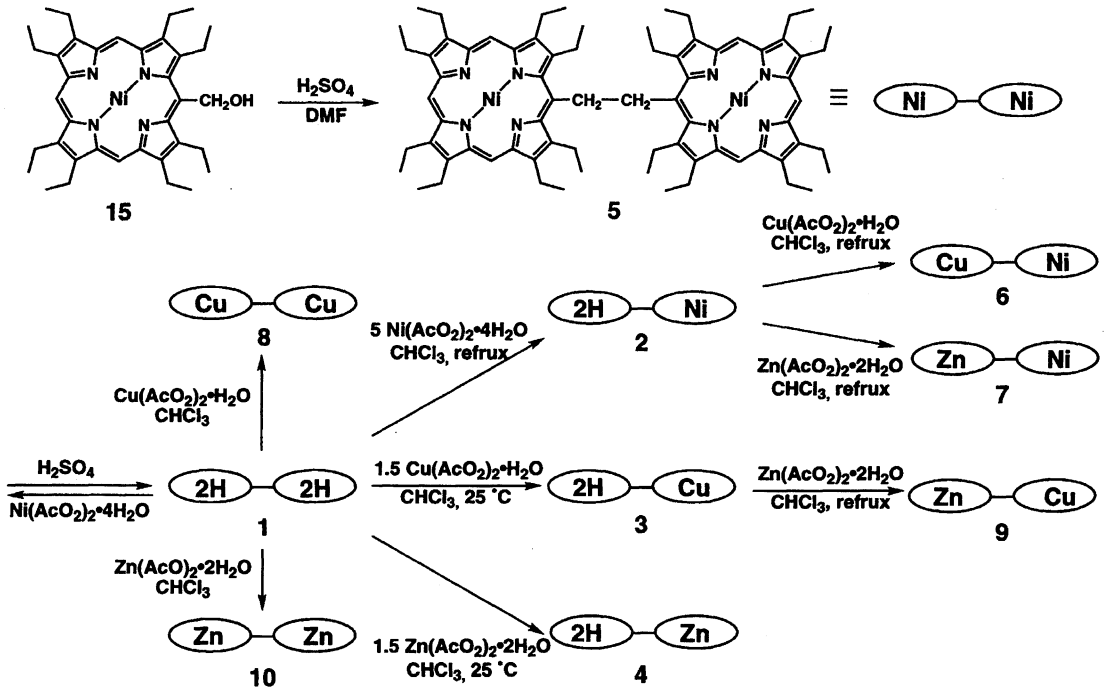

Scheme 1.

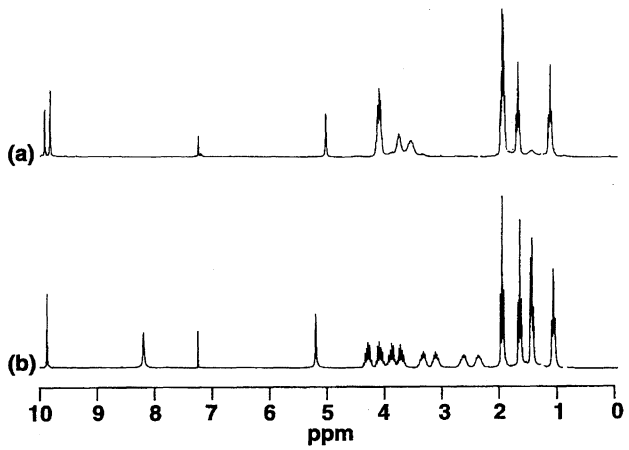

Fig. 2. ^{1}N NMR spectra of 5,5′-ethylenbis(octaethylporphyrin) in $CDCl_3$: (a) **1** ($M^1 = M^2 = 2H$); (b) **10** ($M^1 = M^2 = Zn$).

shift was observed for *meso*-β protons and methylene protons of Et-B (see Fig. 4), compared with **1** and monomer **14**. These characteristics are the same as seen in *cis* isomer of 5,5′-vinylenebis(porphyrin).[22] This clearly indicates that the structure of **10** in solution takes *syn* conformation of face-to-face fashion. On the other hand, chemical shifts and the spin connectivities of the other class of compounds are not so different compared with the corresponding monomers. Therefore, these compounds are assumed to take an *anti* conformation. Selected observed chemical shifts of monomers and dimers are summarized in Table 1.

In order to obtain much information about the structure of the dimers, all the signals of protons in **10** was assigned by using double quantum filtered ^{1}H–^{1}H correlation spectroscopy (DQF-COSY, Fig. 3), truncated driven nuclear Overhauser effect (TOE), and phase sensitive nuclear Overhauser correlation spectroscopy (ph-NOESY). Additionally, the assignments of all the signals of carbons for **10** were also carried out using H–C correlation spectroscopy (H–C COSY), and ^{1}H-

Table 1. Selected ^{1}H NMR Data of Diamagnetic Porphyrin Dimers and Monomers in Chloroform-*d*

	M^1	M^2	Structure	*meso*-α	$(\Delta)^{a)}$	*meso*-β	$(\Delta)^{a)}$	*meso*-α'	$(\Delta)^{a)}$	*meso*-β'	$(\Delta)^{a)}$	N–H
1	2H	2H	*anti*	9.87	(+0.23)	9.79	(+0.31)					−2.83, −3.06
2	2H	Ni	*anti*	9.90	(+0.20)	9.98	(+0.12)	9.56	(+0.20)	9.38	(+0.38)	−2.79, −2.90
4	2H	Zn	*syn*	9.72	(+0.38)	8.71	(+1.39)	9.84	(+0.33)	8.77	(+1.40)	−4.37
5	Ni	Ni	*anti*	9.48	(+0.28)	9.32	(+0.44)					
7	Ni	Zn	*syn*	9.46	(+0.30)	8.70	(+1.06)	9.95	(+0.22)	9.44	(+0.73)	
10	Zn	Zn	*syn*	9.84	(+0.33)	8.17	(+2.00)					
11	2H			10.10								−3.73
12	Ni			9.76								
14	Zn			10.17								

a) Difference in chemical shifts between dimer and corresponding monomer. Plus value implies upfield shifts.

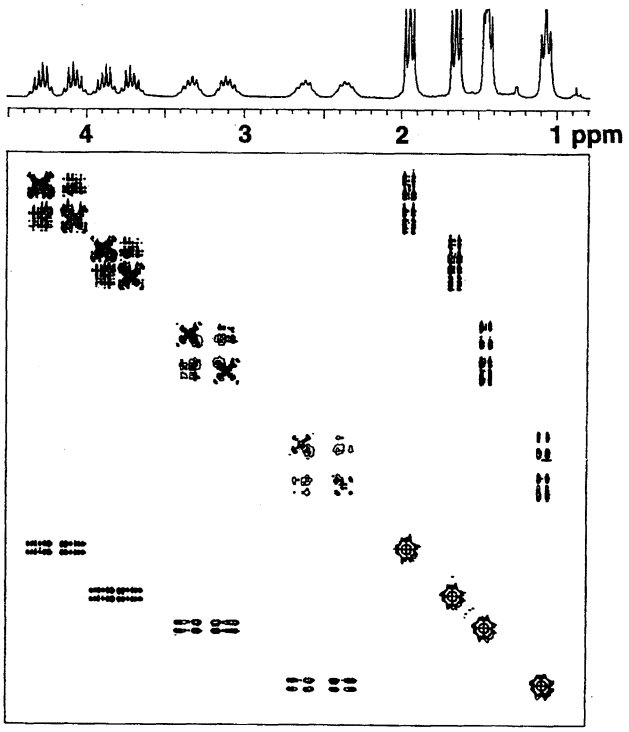

Fig. 3. DQF-COSY spectrum of **10**.

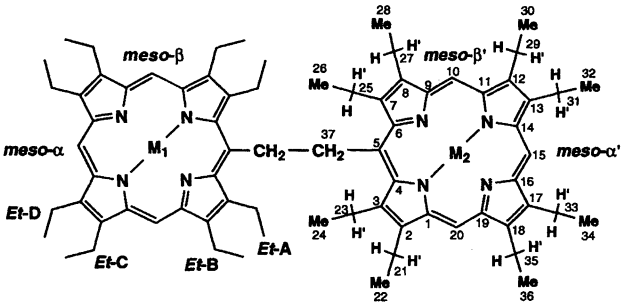

Fig. 4. Numbering of proton and carbon atoms in 5,5′-ethylenbis(octaethylporphyrin).

detected heteronuclear multiple bond connectivity (HMBC).

Four sets of methylene protons of **10** correlate not only with each other, but also with methyl protons in DQF-COSY (Fig. 3). The spectra clearly gave the connectivities of four ethyl groups, Et-A, Et-B, Et-C, and Et-D. NOE, TOE, and ph-NOESY experiments established the positions of the ethyl group in a straightforward manner. All of the protons of **10** correlate with some other protons. Such results are summarized in the experimental section. For instance, H^{15} correlates with $H^{31'}$ and $H^{33'}$, H^{10} and H^{20} correlate with $H^{21'}$, $H^{27'}$, H^{29}, and H^{35}, and so on (Fig. 4). Assignments of all of the carbons with protons were performed by H–C COSY unequivocally. HMBC results confirmed the quartenary carbons and are consistent with the results of other NMR experiments.

Based on the assignments described above, we could determine the structure of the dimers having no central zinc atoms to be *anti* orientation, as described below. Thus, the ethyl group of these compounds show their peaks at higher fields compared with the corresponding monomers and the extent of the upfield shift becomes larger when the ethyl groups locate closer to the center of the molecule (Et-D < Et-C < Et-B < Et-A). Methylene protons of Et-A for **1** were observed at 3.52 ppm and shifted to upfield by 0.59 ppm from the value of **11**. Since the upfield shifts are attributable to the ring current of the other porphyrin ring in a molecule, this behavior in ethyl groups supports *anti* orientation, which was reported for the crystal structure of **5**.[23] On the other hand, the behavior of the upfield shifts of ethyl substituents in **10** (Et-D < Et-C < Et-A < Et-B) is different from those of porphyrin dimers lacking zinc atoms. Thus, the upfield shifts of methylene protons of Et-B in **10** (1.49 and 1.77 ppm) are larger than that of **1** (0.37 ppm). No large differences in the ^{13}C chemical shifts were seen for the same pair. However, the signals of C^2, C^3, C^7, C^8, C^{21}, C^{22}, C^{27}, and C^{28} showed upfield shift (ca. 1.6 ppm) compared with those of **14**.

Multiplicity of methylene signals of ethyl groups gave more information about the structure of the dimers. The pattern of **4**, **7**, and **10** containing at least one zinc porphyrin ring is quite different from that of **1**, **2**, and **5** and resembles the pattern seen in *cis*-5,5′-vinylenebis(porphyrin),[22] where all the methylene protons are splitted into eight sextets. Although these protons of both the *syn*- and *anti*-forms are prochiral, only *syn*-form shows complex signals due to the strong ring current effects of the other porphyrin ring. Similar behavior was reported in cofacial porphyrin dimer[24,25] supporting the present assignment.

In the case of monomeric porphyrins such as octaethylporphyrin and its metal complexes, the chemical shifts of *meso* proton are found at around 10 ppm (Table 1). In dimeric porphyrins **1**, **2**, and **5**, these protons showed their peaks in the similar region. However, the corresponding protons of **4**, **7**, and **10** shifted upfield by more than 1 ppm. A similar upfield shift of *meso* protons was also reported for cofacial coproporphyrin II dimer[26,27] connected by a rigid disulfide bond.[28] Inner N–H protons of Zn–2H complex **4** also show their peaks at higher field (−4.37 ppm), compared with those of **1** and **2** (**1**: −2.83 and −3.06 ppm; **2**: −2.79 and −2.90 ppm). These upfield shifts are additional evidence for the *syn*-form of **4**, **7**, and **10**.

In variable temperature NMR studies of **10**, no change in their shapes was observed even up to 110 °C in chlorobenzene-d_5.

UV-vis and MCD Studies. Since no information was available by NMR concerning the structure of paramagnetic species **3**, **6**, **8**, and **9**, we studied UV-vis, and magnetic circular dichroism (MCD) spectra for all the compounds described above.

The degenerated allowed transitions of a porphyrin $\overline{\Psi}_0 \rightarrow \overline{\Psi}_x$ and $\overline{\Psi}_0 \rightarrow \overline{\Psi}_y$ with transition moments μ_x and μ_y, respectively, interact in the dimer systems as the following, where $\overline{\Psi}_0$ is the wavefunction of ground state and $\overline{\Psi}_x$ and $\overline{\Psi}_y$ are those of excited states.[29] Wavefunctions of excited states interact in four manners and produce four combination states (Figs. 5 and 6), $\overline{\Psi}_x^+$, $\overline{\Psi}_x^-$, $\overline{\Psi}_y^+$, and $\overline{\Psi}_y^-$, where $\overline{\Psi}_x^+$,

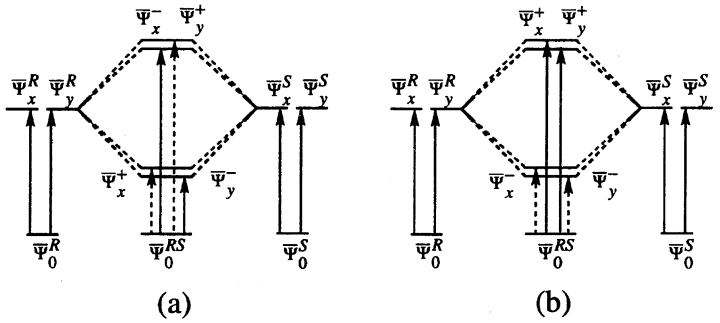

Fig. 5. Exciton band energy diagram for dimer systems. (a) *anti*, (b) *syn* conformation.

$\overline{\Psi}_x^-$, $\overline{\Psi}_y^+$, and $\overline{\Psi}_y^-$ are the following:

$$\overline{\Psi}_y^+ = \frac{1}{\sqrt{2}}\left(\overline{\Psi}_y^R + \overline{\Psi}_y^S\right),$$
$$\overline{\Psi}_y^- = \frac{1}{\sqrt{2}}\left(\overline{\Psi}_y^R - \overline{\Psi}_y^S\right),$$
$$\overline{\Psi}_x^+ = \frac{1}{\sqrt{2}}\left(\overline{\Psi}_x^R + \overline{\Psi}_x^S\right),$$
$$\overline{\Psi}_x^- = \frac{1}{\sqrt{2}}\left(\overline{\Psi}_x^R - \overline{\Psi}_x^S\right).$$

In the *anti*-conformer (in Fig. 5 (a)), transition moments, μ, associated with the transitions to $\overline{\Psi}_x^-$ and $\overline{\Psi}_y^-$ are not zero and allowed (in Fig. 6 (b) and (c)), whereas those of $\overline{\Psi}_y^+$ and $\overline{\Psi}_x^+$ are zero and forbidden (in Fig. 6 (a) and (d)), respectively, and the energy level of $\overline{\Psi}_x^-$ increases and that of $\overline{\Psi}_y^-$ decreases. Therefore, a large excitonic splitting is expected for *anti* conformation. On the other hand, for *syn* conformation, the transitions to energetically close two states, $\overline{\Psi}_x^+$ and $\overline{\Psi}_y^+$, are allowed (in Fig. 6 (e) and (g)) and the transition energy is predicted to be much larger than that of *anti* conformation. Thus, a blue shift is expected (in Fig. 5 (b)).

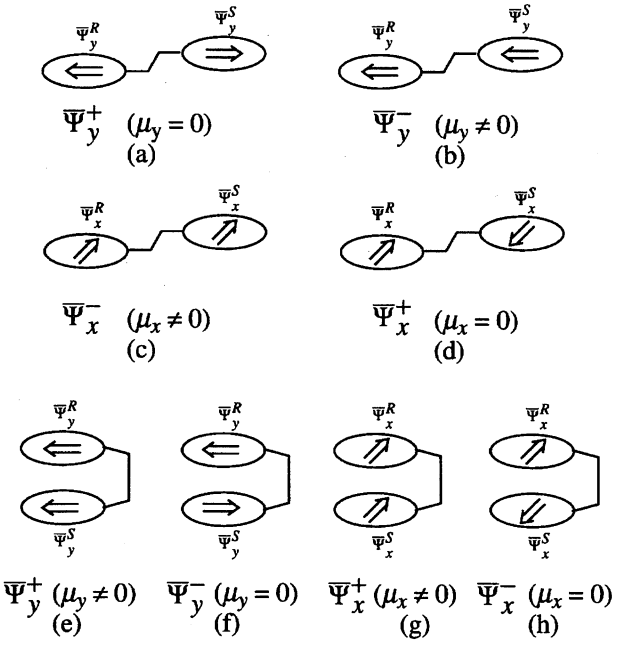

Fig. 6. Interactions of excitons: (a)—(d) *syn* conformation, (e)—(h) *anti* conformation.

Transition moments of the transitions to $\overline{\Psi}_x^-$ and $\overline{\Psi}_y^-$ are zero and forbidden (in Fig. 6 (f) and (h)). Systematic studies support these excitonic theories.[30]

Electronic spectra of **1**—**10** were measured in chloroform (Fig. 7 and Table 2). No distinct tendencies were found in the band shifts ($\Delta\overline{\nu}$) and in the half widths of the peaks related to the structure. The half widths of the broad Soret bands for zinc containing *syn*-complexes (**4**: 3630, **10**: 3760 cm^{-1}) are almost the same as the corresponding value for *anti*-complex (**1**: 3630 cm^{-1}).

In Fig. 8, MCD spectra of typical examples for *anti*-(**5**) and *syn*-(**10**) dimers are shown. The two dimers with C_{2v} or C_{2h} symmetry give rise to MCD spectra consisted of the Faraday B term due to the mixing of the ground and excited states with other electronic states under the influence of the external magnetic field.[31] Values of the peak-trough widths $\Delta\overline{\nu}$ of the Soret band are summarized in Table 2. From the table, $\Delta\overline{\nu}$ value of the zinc complexes **4**, **7**, and **10** are less than 1100 cm^{-1}. Other complexes **1**, **2**, and **5** gave more larger values. The *anti* structures of these complexes are well-characterized by NMR spectra in this study and are confirmed by X-ray analysis.[23] The observed $\Delta\overline{\nu}$ values for the above complexes are consistent with excitonic theory schematically shown in Fig. 5, i.e., *syn* and *anti* conformations give small (<1100 cm^{-1}) and large splittings (>1300 cm^{-1}), respectively. Futhermore, the fact that $\overline{\nu}_1$ of **10** exhibits a blue shift of ca. 300 cm^{-1} as compared with monomeric reference **14**, agrees with the exciton theoretical prediction. The $\Delta\overline{\nu}$ values for the copper containing paramagnetic complexes were 1300 (for **3**), 1800 (for **6**), 1700 (for **8**), and 1100 cm^{-1} (for **9**). Considering the criterion described above, the zinc-containing complex **9** is assumed to be *syn* conformation and others are to be *anti* conformation. The $\Delta\overline{\nu}_1$ of **8** is shifted to shorter wavelength by 1300 cm^{-1} compared with **13** and is also consistent with excitonic theory.

MCD spectra of **4** and **7** display quite unusual absorption shapes compared with others. The $\overline{\nu}_2$ of Soret band splitted into doublet, 25100 and 24400 cm^{-1} for **4**, 24200 and 25500 cm^{-1} for **7**, respectively. However, $\Delta\overline{\nu}$ between $\overline{\nu}_2$ and short wavelength peak of $\overline{\nu}_1$ are both less than 1100 cm^{-1} and those are consistent with the above results.

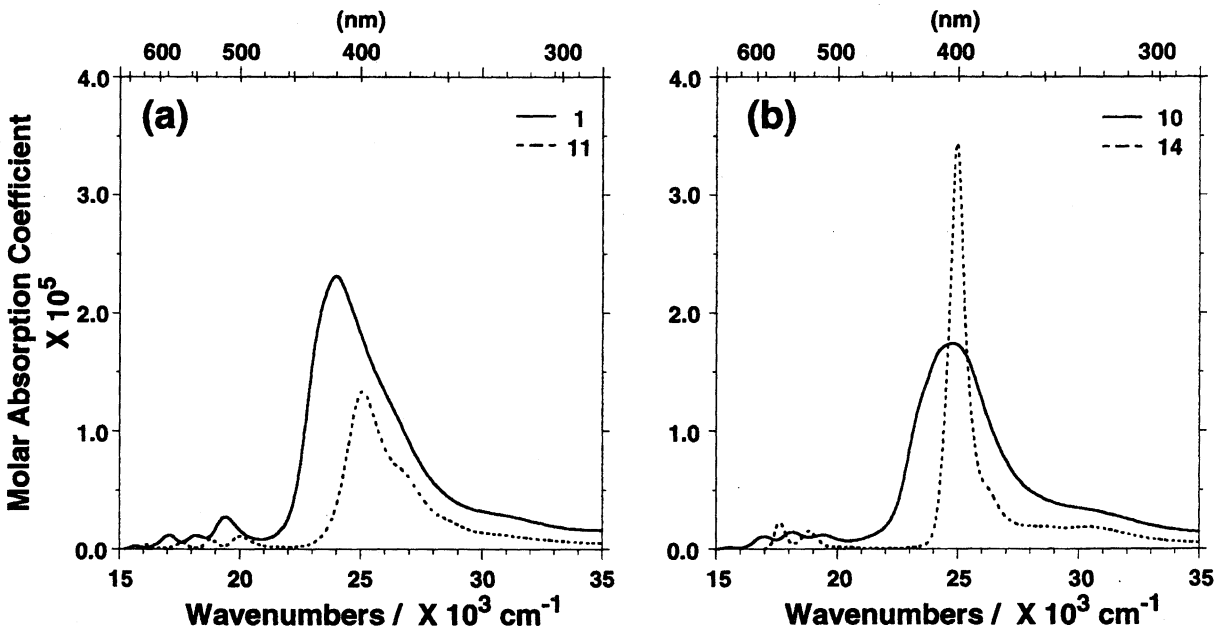

Fig. 7. Absorption spectra in chloroform: (a) **1** (M^1=M^2=2H) and **11** (M=2H); (b) **10** (M^1=M^2=Zn) and **14** (M=Zn).

Table 2. Absorption and MCD Spectral Data of Porphyrin Dimers and Monomers in Chloroform (cm^{-1})

	M^1	M^2	Absorption			MCD		
			Soret-band	Half bandwidth	Q-band	$\overline{\nu}_1$	$\overline{\nu}_2$	$\Delta\overline{\nu}$
1	2H	2H	24010	3630	19420, 18200, 17110, 15670	23000	24300	1300
2	2H	Ni	23810	2700	19420, 18380, 17210, 15700	23100	24700	1600
3	2H	Cu	24390	3370	19400, 18280, 17060, 15650	23300	24600	1300
4	2H	Zn	24810	3630	19460, 18180, 17010, 15630	23300	25100	1800
							24400	1100
5	Ni	Ni	23890	2330	18550, 17420	23800	25100	1300
6	Ni	Cu	23750, 24180	2600	18480, 17440	23600	25400	1800
7	Ni	Zn	23640, 24210	2850	18280, 17380	23300	24200	2200
							25500	900
8	Cu	Cu	25250	2460	18330, 17320	23600	25300	1700
9	Cu	Zn	25280	2070	18180, 17240, 16950	24200	25300	1100
10	Zn	Zn	25220	3760	18080, 17180, 16890	24200	25300	1100
11	2H		25160		18760, 17670, 16850, 16140	24200	25100	900
12	Ni		25540		19400, 18130	25300	26000	700
13	Cu		25190		19120, 17870	24900	25300	400
14	Zn		25030		18850, 17640	24700	25100	400

Discussions and Conclusion

The present results obtained from NMR and MCD spectra clearly show the attractive interactions between two porphyrins overcome the steric repulsion between ethyl substituents when at least one of the two rings is complexed with zinc ion. When neither of the two porphyrin rings are complexed with zinc ion, the interaction between them becomes repulsive. No concentration dependence of the chemical shifts and the low coordinative character of $CDCl_3$ to zinc porphyrins show that this phenomenon is an endogamous property of the molecules.[5] This conclusion is reached, for the first time, by this experiment, although the tendency to aggregate for zinc porphyrins has been reported.[10,32,33]

Such attractive interaction can be explained as follows. Based on the electronic structure of several metalloporphyrins, the net electron population of metals was determined to be +0.40 for Zn, +0.28 for Cu, and +0.30 for Ni.[34] X-Ray photoelectron spectroscopy for 1s orbitals of porphyrin nitrogen atoms also confirmed this tendency.[35] Thus the intramolecular polarization of zinc complex is the largest among the present metalloporphyrins. Qualitatively, this polarization is governed by the electronegativities of metal ions (Zn: 1.6, Cu: 1.9, Ni: 1.8).[36] The strong dipole–dipole interaction arises from this polarization in the case of zinc complexes, when the two rings arrange in slipped stacking like *cis*-5,5′-vinylenebis(porphyrin).[37] The proposed structure of the dimer is shown in Fig. 9. The larger induced negative charge on the porphyrin ligand interacts attractively with the net positive charge on the zinc metal of the other porphyrin

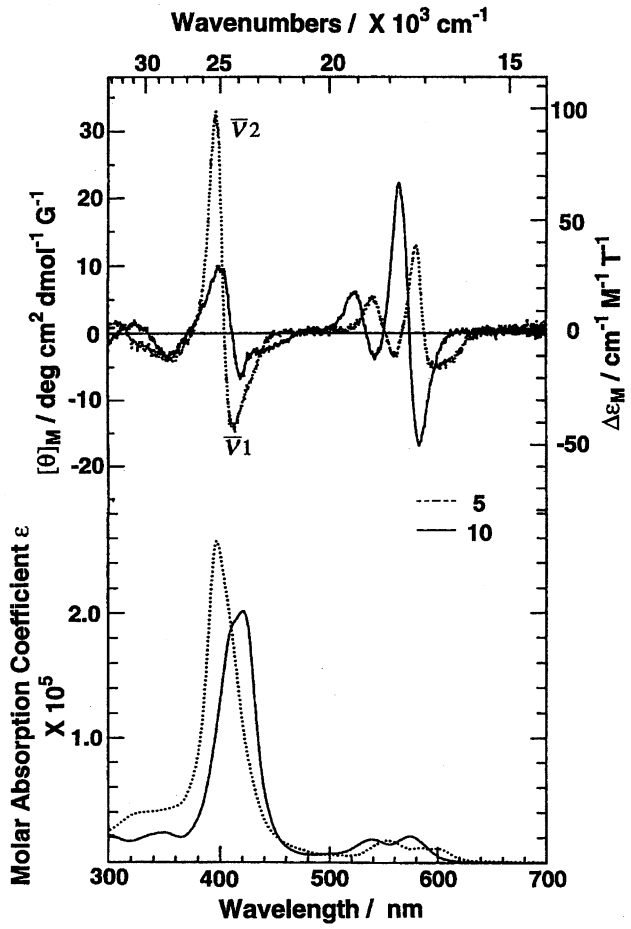

Fig. 8. Absorption and MCD spectra in chloroform of **5** and **10**.

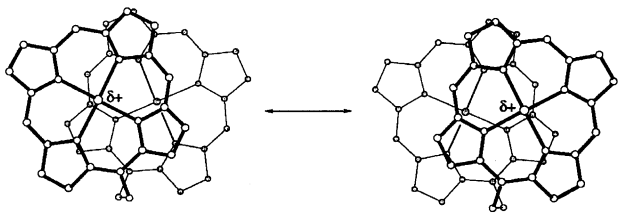

Fig. 9. Proposed structure for zinc-containing porphyrin dimer.

ring. For other metal complexes and free bases, this attractive force is weak and steric repulsive force dominates, so that the *anti* conformation is favored. This electropositive ion-induced polarization effect can explain the other experimental results so far reported. For example, the zinc porphyrin dimer connected by rigid *o*-phenylene linkage shows the characteristic parallel structure[11] and the liquid crystals based on zinc porphyrin show strong intermolecular interactions.[38]

The result in this study may be general for the interaction of porphyrin macrocycles. The strong attractive interactions seem to be one of the most dominant factors for the aggregation of porphyrins, including biological important chlorophyll containing electronegative magnesium ions. The direct observation for the special pair chlorophyll in the photosynthetic reaction center by X-ray analysis[2,39,40] as well as many types of spectral evidence including NMR,[5,32,41–50] IR,[41] and UV-vis.,[8,45,48,50–53] revealed the importance of the coordination bond for dimerization. Where a coordination bond between a magnesium metal of one chlorophyll and the peripheral carbonyl substituent of the other plays an important role. However, π–π interactions seem to be also dominant attractive interactions for the dimerization of chlorophyll, since large polarization is expected for chlorophyll by magnesium metals (electronegativity: 1.2,[36] calculated net positive charge: 0.57[34]).

Recently, the elaborated design and synthesis of porphyrin-based supermolecules are becoming important in the area of contemporary interdisciplinary researches. Our findings clearly explain the intermolecular interactions of metalloporphyrins and have a potential to be used for a new molecular-based architecture and/or advanced materials.

This work was supported by Grants-in-Aid for Scientific Research Nos. 08218239 and 07454166 from the Ministry of Education, Science, Sports and Culture. We are grateful to Wacker Chemicals (East Asia), Co., Ltd., for their generous supply of methyl propionylacetate as a key intermediate for octaethylporphyrin derivatives. We appreciate the technical assistance provided by the Materials Analysis Center of ISIR, Osaka University.

References

1) E. A. Silinsh, "Organic Molecular Crystals," Springer-Verlag, Berlin (1980).
2) J. Deisenhofer, O. Epp, K. Miki, R. Huber, and H. Michel, *J. Mol. Biol.*, **180**, 385 (1984).
3) C. A. Hunter and J. K. M. Sanders, *J. Am. Chem. Soc.*, **112**, 5525 (1990).
4) R. J. Abraham, A. E. Rowan, K. E. Mansfield, and K. M. Smith, *J. Chem. Soc., Perkin Trans. 2*, **1991**, 515.
5) H. Scheer and J. J. Katz, in "Porphyrins and Metalloporphyrins," 2nd ed, ed by K. M. Smith, Elsevier, Amsterdam (1975), p. 493.
6) H. Segawa, H. Nishino, T. Kamikawa, K. Honda, and T. Shimidzu, *Chem. Lett.*, **1989**, 1917.
7) R. F. Pasternack, L. Francesconi, D. Raff, and E. Spiro, *Inorg. Chem.*, **12**, 2606 (1973).
8) H. Tamiaki, S. Takeuchi, R. Tanikaga, S. T. Balaban, A. R. Holzwarth, and K. Schaffner, *Chem. Lett.*, **1994**, 401.
9) P. Leighton, J. A. Cowan, R. J. Abraham, and J. K. M. Sanders, *J. Org. Chem.*, **53**, 733 (1988).
10) Y. Uemori, A. Nakatsubo, H. Imai, S. Nakagawa, and E. Kyuno, *Inorg. Chem.*, **31**, 5164 (1992).
11) A. Osuka, S. Nakajima, T. Nagata, K. Maruyama, and K. Toriumi, *Angew. Chem., Int. Ed. Engl.*, **30**, 582 (1991).
12) A. Osuka, S. Nakajima, and K. Maruyama, *J. Org. Chem.*, **57**, 7355 (1992).
13) S. Jeon, O. Almarsson, R. Karaman, A. Blasko, and T. C. Bruice, *Inorg. Chem.*, **32**, 2562 (1993).
14) D. P. Arnold, A. W. Johnson, and M. Winter, *J. Chem. Soc., Chem. Commun.*, **1976**, 797.
15) D. Arnold, A. W. Johnson, and M. Winter, *J. Chem. Soc., Perkin Trans. 1*, **1977**, 1643.
16) N. Ono, H. Kawamura, M. Bougauchi, and K. Maruyama, *Tetrahedron*, **46**, 7483 (1990).
17) in Ref. 5, p. 795.

18) G. V. Ponomarev and A. M. Shul'ga, SU Patent 1172922 (1985).
19) in Ref. 5, p. 195.
20) R. Guilard, M. A. Lopez, A. Tabard, P. Richard, C. Lecomte, S. Brandes, J. E. Hutchison, and J. P. Collman, *J. Am. Chem. Soc.*, **114**, 9877 (1992).
21) J. S. Lindsey and J. N. Woodford, *Inorg. Chem.*, **34**, 1063 (1995).
22) G. V. Ponomarev, V. V. Borovkov, K. Sugiura, Y. Sakata, and A. M. Shul'ga, *Tetrahedron Lett.*, **34**, 2153 (1993).
23) P. B. Hitchcock, *J. Chem. Soc., Dalton Trans.*, **9**, 2127 (1983).
24) J. W. Buchler, A. D. Cian, J. Fischer, M. Kihn-Botulinski, H. Paulus, and R. Weiss, *J. Am. Chem. Soc.*, **108**, 3652 (1986).
25) Y. Kobuke and H. Miyaji, *J. Am. Chem. Soc.*, **116**, 4111 (1994).
26) P. S. Clezy, D. C. Craig, V. J. James, J. F. McConnell, and A. D. Rae, *Cryst. Struct. Commun.*, **8**, 605 (1979).
27) P. S. Clezy, C. J. R. Fookes, and G. A. Smythe, *Aust. J. Chem.*, **34**, 2595 (1981).
28) M. Aida and C. Nagata, *Theor. Chim. Acta*, **70**, 73 (1986).
29) M. Kasha, H. R. Rawls, and M. A. El-Bayoumi, in "Molecualr Spectroscopy VIII," Butterworths, London (1965), p. 371.
30) A. Osuka and K. Maruyama, *J. Am. Chem. Soc.*, **110**, 4454 (1988).
31) J. C. Sutherland, in "The Porphyrins," ed by D. Dolphin, Academic Press, New York (1978), Vol. 3, p. 225.
32) R. J. Abraham, F. Eivazi, H. Pearson, and K. M. Smith, *J. Chem. Soc., Chem. Commun.*, **1976**, 698.
33) R. J. Abraham, F. Eivazi, H. Pearson, and K. M. Smith, *J. Chem. Soc., Chem. Commun.*, **1976**, 699.
34) M. Zerner and M. Gouterman, *Theor. Chim. Acta*, **4**, 44 (1966).
35) D. H. Karweik and N. Winograd, *Inorg. Chem.*, **15**, 2336 (1976).
36) L. C. Pauling, "The Nature of Chemical Bond," 3rd ed, Cornell University Press, Ithaca (1960), p. 93.
37) M. O. Senge, K. R. Gerzevske, M. G. H. Vicente, T. P. Forsyth, and K. M. Smith, *Angew. Chem., Int. Ed. Engl.*, **32**, 750 (1993).
38) Y. Shimizu, M. Miya, A. Nagata, K. Ohta, I. Yamamoto, and S. Kusabayashi, *Liq. Cryst.*, **14**, 793 (1993).
39) H.-C. Chow, R. Serlin, and C. E. Strouse, *J. Am. Chem. Soc.*, **97**, 7230 (1975).
40) R. Serlin, H.-C. Chow, and C. E. Strouse, *J. Am. Chem. Soc.*, **97**, 7237 (1975).
41) L. J. Boucher and J. J. Katz, *J. Am. Chem. Soc.*, **89**, 4703 (1967).
42) S. G. Boxer, G. L. Closs, and J. J. Katz, *J. Am. Chem. Soc.*, **96**, 7058 (1974).
43) F. K. Fong, *J. Am. Chem. Soc.*, **97**, 6890 (1975).
44) R. P. H. Kooyman and T. J. Schaafsma, *J. Am. Chem. Soc.*, **106**, 551 (1984).
45) D. Brune, T. Nozawa, and R. E. Blankenship, *Biochemistry*, **26**, 8644 (1990).
46) R. J. Abraham, D. A. Goff, and K. M. Smith, *J. Chem. Soc., Perkin Trans. 1*, **1988**, 2443.
47) R. J. Abraham, A. E. Rowan, D. A. Goff, K. E. Mansfield, and K. M. Smith, *J. Chem. Soc., Perkin Trans. 2*, **1989**, 1633.
48) T. Nozawa, K. Ohtomo, Y. Morishita, H. Konami, and M. T. Madigan, *Chem. Lett.*, **1992**, 261.
49) R. J. Abraham, A. E. Rowan, N. W. Smith, and K. M. Smith, *J. Chem. Soc., Perkin Trans. 2*, **1993**, 1047.
50) T. Nozawa, K. Ohtomo, M. Sozuki, Y. Morishita, and M. T. Madigan, *Bull. Chem. Soc. Jpn.*, **66**, 231 (1993).
51) F. Bobe, W. N. Pfennig, K. L. Swanson, and K. M. Smith, *Biochemistry*, **29**, 4340 (1990).
52) F. K. Fong and V. Koester, *J. Am. Chem. Soc.*, **97**, 6888 (1975).
53) H. Tamiaki, T. Miyatake, R. Tanikaga, A. R. Holzwarth, and K. Schaffner, *Angew. Chem., Int. Ed. Engl.*, **35**, 772 (1996).